Synchronous dynamics of spectral greening trends and regional climate variability across Europe

Michael Kempf (michael.kempf@geographie.uni-freiburg.de)
University of Freiburg: Albert-Ludwigs-Universitat Freiburg https://orcid.org/0000-0002-9474-4670

Research Article

Keywords: NDVI, greening trend, climate change, drought, landcover change, spatial modelling

Posted Date: April 5th, 2022

DOI: https://doi.org/10.21203/rs.3.rs-1457891/v1

Abstract

Europe witnessed a strong increase in climate variability and extremes over the past decades that caused degradation of ecological and societal resilience. Cascading feedbacks like the 2003 and 2010 heat waves were considered environmental response to anthropogenically reinforced climate anomalies. Land-use intensification, landcover change, and forest degradation further increased the pressure on the ecosystem's functionalities. Conversely, recent satellite observations emphasized positive vegetation and landcover reflectance trends as a response to rising atmospheric CO input and global warming, particularly in the northern latitudes. However, these global trends obfuscate the intensified regional divergence of climate variability and extremes and risk underestimating future climate induced feedbacks. Consequently, long-term climate trends and variability must be analysed together with annual and interannual anomalies to understand regional feedback mechanisms and surface cover changes. This article presents long-term NDVI (Normalized Difference Vegetation Index) monthly time series analyses compared to multicomponent environmental background variability to highlight European-scale greening trends over the period 2001–2020. Significant warming and persistent hot droughts affect regional vegetation trends in central Europe compared to prolonged phenological phases and reduced snow-cover in north-eastern Europe.

1 Introduction

Droughts are among the most severe environmental disasters, enhancing ecological and socio-economic conflicts (Geist and Lambin 2004; Godfray et al. 2010; Gupta et al. 2020; Kaczan and Orgill-Meyer 2020; Lambin and Geist 2006; Lesk et al. 2016; Schmidhuber and Tubiello 2007; Xu et al. 2020). Particularly long-term drought spells, hot drought events, and mega-heatwaves like in 2003 and 2010 provoke persistent landcover transformations that amplify faunal and floral aggravation and desertification processes, and force socio-cultural adaptation (Barriopedro et al. 2011; Fischer et al. 2021; Lin et al. 2020; Luterbacher et al. 2004; Miralles et al. 2014; Pereira et al. 2017; Quesada et al. 2012; Rasmijn et al. 2018; Schumacher et al. 2019; Sousa et al. 2020; Zhou et al. 2019). Human-induced surface degradation from crop production and extensive cattle breeding further contributes to current landcover changes (Burrell et al. 2020; Harris 2010). Parallel to this, however, the number of severe flood events and the frequency of wet spells increased over the past decades with significant regional variability across Europe (Breinl et al. 2020; Dai et al. 1998; Dietze et al. 2022; Zolina et al. 2010). The development of rapidly occurring and long-lasting extremes poses particularly high challenges on the ecosystem's adaptive mechanisms. Due to the accelerated speed, intensification, and persistence of dry and wet spell transitions, severe water shortages or massive oversupply occur within short term periods. Recent results by Fischer et al. (2021) emphasized the strong increase in climate extremes probability and the short return periods of record-shattering events during the forthcoming decades (Fischer et al. 2021).

Parallel to this, satellite observations and vegetation response monitoring detected enhanced global spectral greening and a generally positive trend in surface reflectance patterns, which showed that previously degraded landscapes were affected by anthropogenic signals superimposed on causative

precipitation trends (Cortés et al. 2021; Forzieri et al. 2017; Herrmann et al. 2005; Myers-Smith et al. 2020; Piao et al. 2020). Apparently, complex and scale-dependent vegetation response to global warming is strongly coupled to regional climatic feedbacks and topographic variables (Forzieri et al. 2017; Myers-Smith et al. 2020; Piao et al. 2020). Whereas anthropogenic reinforcements of spectral greening trends are most likely linked to intensified land-use management (Chen et al. 2019; de Jong et al. 2012; Piao et al. 2020). Crop production accounts for over one third of the green-leaf area increase, highlighting the spatial and seasonal variability of global greening trends (Chen et al. 2019; Winkler et al. 2021). Extensive monoculture cultivation, on the other hand, increases the yield vulnerability to climate extreme events and persistent heat waves, which in turn causes massive harvest loss (Brunner et al. 2018; Gampe et al. 2021). A general spectral greening trend is likely to obfuscate regional vegetation response anomalies during persistent drought periods and to underestimate local environmental feedbacks. In general, the increase in globally observed surface reflectance is biased by multiple components, including latitudinal gradients and snow cover variability, wildfire development, land-use strategies, and forest decline – making it particularly difficult to trace regional response to global warming on the continental scale. For this reason, long-term trend observation of surface reflectance patterns through remote sensing tools can provide a suitable resource to evaluate global impacts of climate change feedbacks. However, tracing regional ecosystem response models must include annual and interannual anomaly detection to highlight the increase of annual variability masked by overall trends.

This paper evaluates multiannual greening trends, regional vegetation response, and surface cover reflectance anomalies across Europe using long-term monthly vegetation indices (NDVI) and monthly climate and environmental variables (Beaudoing et al. 2020; Harris et al. 2020; Kumar et al. 2006; Peters-Lidard et al. 2007; Rodell et al. 2004) (Table 1). Monitoring vegetation change through remote sensing techniques has become a common tool since the introduction of the NDVI and the availability of medium resolution satellite imagery covering the past two decades (Cortés et al. 2021; Tucker 1979; Tucker et al. 1986). Monthly MODIS (Moderate Resolution Imaging Spectroradiometer) NDVI imagery were analysed to detect vegetation anomalies compared to background spectral greening and browning trends, precipitation and temperature variability and environmental covariates over the period 2001–2020. Rank-based correlation between environmental variables and NDVI time-series was performed to test the predictive models for significant interdependencies between climate variables and landcover change. Eventually, the models were compared to annual and monthly anomalies to detect regional feedbacks and to highlight the strong temporal variability of dry and wet spells underlying vegetation signals of spectral greening and browning as well as surface reflectance trends across Europe.

2 Material And Methods

The analyses span the period between January 2001 and December 2020. Spatial and temporal subsets of NDVI imagery and environmental parameters from the CRU (Climate Research Unit) (Harris et al. 2020) and GLDAS (Global Land Data Assimilation System) (Beaudoing et al. 2020) datasets were chosen to highlight vegetation response to climate change on a multiscale and multiparameter level. Corine landcover data (CLC) (https://land.copernicus.eu/pan-european/corine-land-cover, last accessed, 26th of

October 2021) was used to measure the degree of surface transformation and to compare trends over cropland and forest cover. Annual, seasonal, and monthly vegetation anomalies were calculated for each spatial and temporal subset. Growing season differentiations in NDVI were calculated for the periods March-May (MAM), June-August (JJA), September-November (SON), and December-February (DJF, including December 2000). All temporal and spatial subsets were analysed for vegetation anomalies and spectral greening and browning trends based on the MODIS NDVI time-series with 240 single images. The NDVI is a method to measure vegetation vigour from satellite imagery and acts as a vegetation performance indicator where higher values indicate higher photosynthetic activity (Justice et al. 1985; Tucker 1979). Vegetation indices are used to distinguish photosynthetic activity of vegetation from other land surfaces. The index is based on the reflection characteristics of near infrared (NIR) and the absorption of red radiation (Red) (Anyamba and Tucker 2005; Tucker 1979; Tucker et al. 1991). All statistical analyses were performed using the R-environment (R: A language and environment for statistical computing. R Foundation for Statistical Computing, Vienna, Austria. URL https://www.R-project.org/). All code underlying the analyses are stored as supplementary data to this article.

2.1 MODIS NDVI monthly dataset

To measure the relationship between temporal variability of climate variables, geographical location, and vegetation feedback, a global NDVI monthly time series dataset (2000–2020) was downloaded from the Earthdata server of the United States Geological Survey (USGS) (https://lpdaac.usgs.gov/products/mod13c2v006/, last accessed 16th of April 2021) (Didan 2015). The NDVI data consist of cloud-free composites with 0.05° geographic grid resolution (5,600 m), covering the period 02/2000–12/2020 at a monthly return period. The data comes in HDF4 file format (hierarchical data format), which stores scientific data into various subsets and can be read, classified, and saved as single files using the R code from the supplementary data (Code_1). Annual composites, annual mean, and growing season subsets were calculated and cropped to the extent of the study area, defined as the extent of the European coastline vector (available from the EEA (European Environment Agency, https://www.eea.europa.eu/data-and-maps/data/eea-coastline-for-analysis-1/gis-data/europe-coastline-shapefile/at_download/file, last accessed 26th of October 2021). All spatial features < 10^6 m² and parts of Africa and the polar region were removed from the mask layer. The shapefiles are stored as auxiliary data to this article. Code_3 reprojects and crops the extracted MODIS single files to the extent of the study area.

2.2 CRU climate datasets

Multiannual average monthly total precipitation and temperature (2001–2020) was accessed via the data portal of the Climate Research Unit (CRU) of the University of East Anglia (https://crudata.uea.ac.uk/cru/data/hrg/cru_ts_4.05/cruts.2103051243.v4.05/pre/, last accessed 26th of October 2021) (Harris et al. 2020). The .nc files were extracted to single raster datasets using the R-package *ncdf4* (Pierce 2019) and the code available to this article (Code_2). Annual sums were created and anomalies (Code_4) as well as trend analyses were performed (Code_5).

2.3 Global Land Data Assimilation System (GLDAS)

GLDAS climate and environmental datasets were downloaded from the Goddard Earth Sciences Data and Information Services Center (GLDAS Noah Land Surface Model L4 monthly 0.25 x 0.25 degree V2.1 (GLDAS_NOAH025_M, https://disc.gsfc.nasa.gov; last accessed 17th of December 2021) (Beaudoing et al. 2020; Rodell et al. 2004). The .nc files from January 2001 to December 2020 were extracted and stored as annual sums. Trend analysis and anomalies were calculated for annual sums covering the period 2001–2020. Variables underlying the analysis are listed in Table 1.

Tab. 1: GLDAS (Global Land Data Assimilation System, Version 2) variables and units (Beaudoing et al. 2020; Kumar et al. 2006; Peters-Lidard et al. 2007; Rodell et al. 2004).

	Variable id	Standard name	Long name	Unit
GLDAS variables	Evap_tavg	water_evaporation_flux	Evapotranspiration	kg m-2 s-1
	Qs_acc	surface_runoff_amount	Storm surface runoff	kg m-2
	Qsm_acc	surface_snow_melt_amount	Snow melt	kg m-2
	SWE_inst	surface_snow_amount	Snow depth water equivalent	kg m-2
	SnowDepth_inst	surface_snow_thickness	Snow depth	m
	SoilMoi0_10cm_inst	soil_moisture_content	Soil moisture	kg m-2
	SoilMoi10_40cm_inst	soil_moisture_content	Soil moisture	kg m-2
	SoilMoi40_100cm_inst	soil_moisture_content	Soil moisture	kg m-2
	SoilMoi100_200cm_inst	soil_moisture_content	Soil moisture	kg m-2
	SoilTMP0_10cm_inst	soil_temperature	Soil temperature	K
	SoilTMP10_40cm_inst	soil_temperature	Soil temperature	K
	SoilTMP40_100cm_inst	soil_temperature	Soil temperature	K
	SoilTMP100_200cm_inst	soil_temperature	Soil temperature	K
	PotEvap_tavg	potential_evaporation_flux	Potential evaporation rate	W m-2
	ECanop_tavg	evaporation_flux_from_canopy	Canopy water evaporation	W m-2
	Tveg_tavg	transpiration_flux_from_veg	Transpiration	W m-2
	ESoil_tavg	evaporation_flux_from_soil	Direct Evaporation from Bare Soil	W m-2
	RootMoist_inst	root_zone_soil_moisture	Root zone soil moisture	kg m-2
	CanopInt_inst	canopy_water_amount	Plant canopy surface water	kg m-2
	Wind_f_inst	wind_speed	Wind speed	m s-1

Source: Climate Data Interface, version 1.9.8. (https://mpimet.mpg.de/cdi), GLDAS_NOAH025_M: Land Surface Model L4 monthly 0.25 x 0.25 degree V2.1; Rodell et al. (2004), https://doi.org/10.1175/BAMS-85-3-381; Kumar et al. (2006), https://doi.org/10.1016/j.envsoft.2005.07.004; Peters-Lidard et al. (2007), https://doi.org/10.1007/s11334-007-0028-x

2.4 Corine landcover classification

CLC datasets were downloaded from the Copernicus server (https://land.copernicus.eu/pan-european/corine-land-cover, last accessed, 26th of October 2021). The raster data was reprojected to WGS84 EPSG:4326 at a resolution of 0.05°. The CLC legend was acquired from the European Environment Agency (EEA) (https://www.eea.europa.eu/data-and-maps/data/corine-land-cover-2/corine-land-cover-classes-and/clc_legend.csv, last accessed, 26th of October 2021) and the grid codes were extracted for each surface type, which distinguish artificial built-up (1–11), agricultural areas (12–22), and forest cover and semi-natural areas (23–34). Cropland, and forest/semi-natural areas of each year were vectorized and used as mask layers to crop the annual NDVI raster. The mask layers are stored as auxiliary data to this article.

2.5 Anomaly calculations

The arithmetic mean (m) and the first standard deviation (SD) were calculated from aggregated raster stacks (Code_4). SD was subtracted from and added to the mean value (m-SD; m + SD) to create the range of the standard deviation for the reference period. The (m + SD) was subtracted from each single year and growing period value and all values ≤ 0 were removed for the upper limits of the standard deviation range. According to the lower limits of the standard deviation range, (m-SD) was subtracted from each year and growing period value and all values ≥ 0 were removed. Both parts were merged to show negative and positive trends, compared to the long-term temporal series of 20 years (Code_4 and Code_7).

2.6 Raster trend analysis

A time series analysis was conducted using a pixel-wise raster analysis on monthly NDVI, precipitation, temperature, and GLDAS data to detect trends in vegetation change and explanatory covariates (Brandt et al. 2014) (Code_5). For annual greening/browning trend analysis, monthly data was aggregated to annual sums and the slope was calculated to identify trends. P-values were extracted and all values > 0.05 (0.5) were masked to highlight a confidence level of 95% (50%). Analogue NDVI analyses were run on a monthly and seasonal basis and for different climate zones (Beck et al. 2018) as well as for crop production areas, natural forests, and topographic parameters with 500 m ranges to highlight regional and zonal vegetation trends. Boxplots and density curves of NDVI trends with 95% confidence level visualize multiannual, seasonal, and monthly greening and browning trends across Europe. Temperature, Precipitation, and GLDAS variables were equally processed and are stored as supplementary data to this article.

2.7 Rank-based pair-wise correlation

To correlate time-series trend parameters, the variables were packed into raster stacks using monthly totals and annual sums. Due to different spatial resolution, the NDVI stacks were cropped to the extent of the CRU/GLDAS datasets and resampled to a 0.5°x0.5° resolution. The Spearman rank-based correlation method was chosen to perform pair-wise correlation between NDVI and each environmental variable over the period 2001–2020 (Code_6). The code returns a set of raster layers of correlation values.

3 Results

3.1 Vegetation response to global warming across Europe

NDVI trend analyses over the period 2001–2020 highlight regional vegetation and landcover change as response to climate variability in Europe (Fig. 1). Particularly strong vegetation greening and positive surface reflectance trends can be detected in central, southern, and towards the north-eastern parts of Europe. Western Europe and large parts of France, the Iberian Peninsula, Italy, and the British Islands show weaker but still significant greening. Eastern Europe shows a strongly negative vegetation response to climate variability and an increasing browning trend with significant peaks in south-eastern Ukraine and Russia. The strong greening trends of northern and eastern Europe match the temperature trends of

the region during the past 20 years. Due to feedback mechanism of global warming and heat waves, the snow cover over northern Europe is decreasing, which influences the surface reflectance patterns indicating positive greening trends. These are, however, more likely to represent reduced snow cover in spring (Bormann et al. 2018; Dye and Tucker 2003; Zhang et al. 2020). Less and scattered as well as darkened snow cover resulting from particle deposition further amplifies solar heating of snowpacks and contributes to increased snow melt (Flanner et al. 2009). During spring, these interactions can lead to changes in surface reflectance that are not caused by an earlier onset of the phenological phase but by removed or scattered snow cover (Dye and Tucker 2003). Reverse browning trends, on the other hand, can be linked to enhanced fire activity (Eckert et al. 2015; Forkel et al. 2013).

In general, significant warming can be detected in most parts of continental Europe and particularly in the central and north-eastern parts. A strong increase in total precipitation further amplifies vegetation response in north-eastern Europe and large parts across Turkey, Greece, and toward the Black Sea. However, parts of central Europe show continuous greening signals despite increasing temperature and decreasing precipitation trends. Continental eastern Europe is more directly related to drying-up and increasing temperature trends.

Considering European vegetation response to climate change mechanisms on multiannual scales, a monthly, seasonal, and regional variability in trend behaviour can be detected. Particularly positive reflectance trends occur during November and December, which emphasize the strong temperature increase and a shift in snow cover duration in north-eastern continental climate zones (Fig. 2). A very strong warming signal during February further decreases snow cover and enhances the positive spectral reflectance (Fig. 3). The region shows constant greening throughout spring and summer, compared to a significant browning trend in eastern Europe and France and a less significant greening in central Europe. Browning trends increase significantly during September and October, affecting large parts of central-eastern and western Europe. Particularly the western part shows negative vegetation response, which can be traced back to strong negative precipitation trends and an increase in mean temperature from July onwards (Fig. 4). An increase in winter heavy precipitation has been predicted in western Europe for future climate models, particularly affecting the UK and parts of south-western Scandinavia (Chan et al. 2018; Christidis et al. 2021; Ketzler et al. 2021; Whan et al. 2020). The simulated increase in winter precipitation is predominantly visible during December, whereas spring and early summer rainfall decreases significantly. Despite the changes in mean precipitation trends, the annual variability strongly increases, confirming recent results (Chan et al. 2018; Zhang et al. 2021).

3.2 Correlation and attribution of climatic variables to spectral greening

Spatial correlation between temperature and landcover reflectance patterns shows strong significance with increasing temperatures and vegetation response across central and north-eastern Europe (Fig. 5). Precipitation trends are not significant in the north-eastern part and the increasing spectral greening signal is linked to the temperature trends and reduced snow coverage (Fig. 6). Soil moisture correlates

positively with enhanced vegetation response but is spatially connected to a significant increase in precipitation. Eastern Europe and southern Russia and Ukraine show significantly positive correlation between precipitation and soil moisture decrease, and increased browning trends. The eastern parts of the Black Sea, however, reveal reverse correlation.

In central Europe, and particularly across Germany and central France, regional warming correlates strongly with increased greening trends. But vegetation response is negatively connected to the drying-up process and a very significant decrease in annual total precipitation stands against the positive spectral greening. Here, the monthly variability shows more positive feedbacks. In the southern parts of Europe, the correlation is regionally diverse. In central and southern Italy and Spain, total precipitation is strongly decreasing, which is not entirely mirrored in the greening trends – probably linked to growing irrigation measures (Cramer et al. 2018; Pool et al. 2021). Soil temperature and evapotranspiration are strongly increasing, and soil moisture and canopy surface water show negative trends, particularly affecting the infiltration rate and the deeper soil layers (see supplementary data to this article for trend analyses of GLDAS variables).

3.3 Trends in European climate variability and extremes

Recently, the discussion about cause and effect of the local and regional anthropogenic overprint on the ecosystem's functionalities, fuelled by global climate change feedbacks, has been reinforced by the severe gradient of continental European flooding and drought spells (Ciais et al. 2005; Harris 2010; Herrmann and Hutchinson 2005; Lin et al. 2020; Zahradníček et al. 2015). Particularly the severe drought episodes of 2003, 2010, and between 2018 and 2020, followed by dramatic flooding events across Europe in summer 2021, have entered the political and economic debate (Brun et al. 2020; Büntgen et al. 2021; Cramer et al. 2018; Dirmeyer et al. 2021; Hari et al. 2020; Kahle et al. 2022; Kempf and Glaser 2020). Temperatures are constantly increasing across Europe and particularly over terrestrial surfaces. According to the 2021 IPCC report, the year 2020 has been marked the warmest on instrumental record (Masson-Delmotte et al. 2021), which contributes to the enhanced temperature trend of the observation period presented in this article. Compared to the IPCC, the past two decades show stronger regional trend variability, e.g. across the Iberian Peninsula, that demonstrates less positive temperature trends than over the reference period 1960–2020 used by the IPCC (Masson-Delmotte et al. 2021). Temperature anomalies, on the other hand, are less variable here with a tendency towards more hot year anomalies compared to colder events (Fig. 7). Precipitation anomalies, however, increase in both, positive and negative annual sums, and subsequent hot and dry year periods are expected to occur more frequently by the mid of the 21st century (Gampe et al. 2021; Vogel et al. 2021).

The strongest occurrence in positive temperature anomalies can be detected across Turkey, central France, south-western Germany, and extensive parts of Belarus, Ukraine, and Russia. In addition to this, negative temperature anomalies are lacking, which underlines the trend towards prolonged hot drought periods and strongly increasing annual average temperatures – affecting tree growth and enhance increased die-back (Del Martinez Castillo et al. 2022). Across northern Russia, both, positive and negative temperature anomalies are frequent and negative anomalies prevail in the Balkans, which strengthen the

risk of crop failure during periods of either hot droughts or intensified cold waves (Piticar et al. 2018; Vogel et al. 2019). Regional temperature extremes are furthermore accompanied by growing negative precipitation anomalies, particularly across central Europe, the Adriatic, north-western parts of the Iberian Peninsula, and the Alpine region. Where no negative anomalies prevail, a trend towards lower precipitation rates poses a particular threat to regional croplands and the water balance of the forests and meadows. Across central Europe, NDVI anomalies show strongly negative and only partly positive occurrences, which stand against the rising spectral greening trend over the reference period. Accumulated anomalies are rather attributed to increasing numbers of drought periods and clearly indicate the rapidly rising vulnerability of vegetation response to an increase in extreme weather patterns.

4 Discussion And Conclusion

Extreme heatwaves as in 2003 in central Europe and in 2010 over Russia have been traced back to atmospheric patterns that caused a massive increase in surface temperature (Di Capua et al. 2021; Liu et al. 2020). Constant warming over an increasingly desiccated land surface caused persistent thick hot-air masses that maintained surface warming and led to further heat accumulation and soil desiccation, amplifying the heatwave cascading effects (Christian et al. 2020; Miralles et al. 2014). Particularly the southern parts, which experience a significant increase in heat supply and soil temperature and a strong reduction in soil moisture are currently the most productive and intensely exploited wheat cultivation areas (Di Paola et al. 2018). Considering the trend toward increased soil moisture availability and temperature across the northern and north-eastern parts of the country, the land-use patterns are most likely to shift in the future. This can cause strong surface transformation and a reverse trend in soil moisture availability under rapidly increasing surface and soil temperature.

The observed response in plant growth and composition, and a shift towards arid-tolerant species does not necessarily mean a recovery in total ecological diversity (Herrmann and Tappan 2013; Ibrahim et al. 2018; Zida et al. 2020). Partly, this trend is attributed to increased atmospheric CO_2 concentration, precipitation totals, the spread of agricultural exploitation, and increased warming of the permafrost in the Northern Hemisphere (Peng et al. 2020; Piao et al. 2020; Winkler et al. 2021). Global spectral greening trends and phenological shifts over the past two decades were thought to emerge from increased greenhouse gas concentrations and higher temperatures, causing higher biological activity and intensified carbon sink in higher latitudes in the Northern Hemisphere (de Jong et al. 2012; Menzel et al. 2020; Piao et al. 2019; Rosbakh et al. 2021; Zhou et al. 2001). Results from high-resolution satellite LAI (Leaf Area Index) analyses identified forest regrowth following land abandonment as main driving factor of EU-wide spectral greening (Buitenwerf et al. 2018). On the other hand, grassland and shrubs were particularly affected by an inverse trend and according to de Jong and colleagues (2012), semi-arid regions are more vulnerable to browning trends after rapid greening caused by short-term climate variability (de Jong et al. 2012). In combination with persistent hot drought periods, the carbon uptake can be drastically reduced by decreased gross primary production (GPP), particularly affecting grassland and cropland in the northern temperate climate zone (Gampe et al. 2021). General grassland and

cropland response to CO_2 increase is particularly sensitive to soil moisture availability, soil type and texture (Fay et al. 2012) and an increasing soil moisture trend across north-eastern Europe correlates with strong greening signals and reduced snow cover – indicating positive surface reflectance trends. Climate variability and particularly the precipitation rate after the growing season of the preceding year until August of the current year has been shown to control productivity patterns (Li et al. 2013). Recent results have further narrowed down the temporal corridor of European species' phenology during spring and summer to the previous months (Menzel et al. 2006; Wu et al. 2021) – which emphasizes the cause and effect in vegetation response to soil moisture and precipitation deficits during persistent heat waves in warm-dry regions (Klesse et al. 2018). Particularly the Mediterranean suffers from decreasing precipitation trends and rising temperatures. Cramer et al. (2018) highlighted the strong coupling of temperature increase and potential precipitation decline of up to 30% by 2080, accompanied by a 10–20% increase in heavy rainfall events (Cramer et al. 2018) and an increase in heat wave related harvest loss of 3%/yr (Brás et al. 2021). In addition, Winkler et al. (2021) emphasized the strong latitudinal gradient of climate change effects on biomes and highlighted the linkages between northern greening and warming trends compared to southern precipitation variability and subsequent browning (Winkler et al. 2021). Parallel to this, the number of extreme years with heat waves or pronounced cold spells is growing, which will raise questions regarding a calculable risk of future agricultural strategies. Central Europe is particularly affected, showing a strong increase in negative vegetation anomalies, which are explained by the increase in mean annual temperature and the decrease in total precipitation. These trends will intensify in the future and a reversal of the greening trend in the wake of prolonged droughts could lead to massive surface atmosphere-interactions and regional climate amplifications. Further trend analyses of climate variables are needed to enhance the knowledge of regional environmental feedbacks. Monitoring surface transformations over long temporal periods is mostly limited by the scale and detailed ground-based measurements can be carried out only locally, which produces high spatial resolution datasets but lacks the comparison of global environmental response to global feedbacks (Cortés et al. 2021).

Declarations

Code availability

All code underlying the analyses are available as supplement data to this article.

Data availability

All data underlying the results of this article are publicly available on the internet.

Competing interests statement

The author declares no conflict of interest

The author has no relevant financial or non-financial interests to disclose

Funding information

xxx

References

1. Anyamba A, Tucker CJ (2005) Analysis of Sahelian vegetation dynamics using NOAA-AVHRR NDVI data from 1981–2003. J Arid Environ 63:596–614. https://doi.org/10.1016/j.jaridenv.2005.03.007
2. Barriopedro D, Fischer EM, Luterbacher J, Trigo RM, García-Herrera R (2011) The hot summer of 2010: redrawing the temperature record map of Europe. Science 332:220–224. https://doi.org/10.1126/science.1201224
3. Beck HE, Zimmermann NE, McVicar TR, Vergopolan N, Berg A, Wood EF (2018) Present and future Köppen-Geiger climate classification maps at 1-km resolution. Sci Data 5:180214. https://doi.org/10.1038/sdata.2018.214
4. Bormann KJ, Brown RD, Derksen C, Painter TH (2018) Estimating snow-cover trends from space. Nat Clim Chang 8:924–928. https://doi.org/10.1038/s41558-018-0318-3
5. Brandt M, Romankiewicz C, Spiekermann R, Samimi C (2014) Environmental change in time series – An interdisciplinary study in the Sahel of Mali and Senegal. J Arid Environ 105:52–63. https://doi.org/10.1016/j.jaridenv.2014.02.019
6. Brás TA, Seixas J, Carvalhais N, Jägermeyr J (2021) Severity of drought and heatwave crop losses tripled over the last five decades in Europe. Environ Res Lett 16:65012. https://doi.org/10.1088/1748-9326/abf004
7. Breinl K, Di Baldassarre G, Mazzoleni M, Lun D, Vico G (2020) Extreme dry and wet spells face changes in their duration and timing. Environ Res Lett 15:74040. https://doi.org/10.1088/1748-9326/ab7d05
8. Brun P, Psomas A, Ginzler C, Thuiller W, Zappa M, Zimmermann NE (2020) Large-scale early-wilting response of Central European forests to the 2018 extreme drought. Glob Chang Biol 26:7021–7035. https://doi.org/10.1111/gcb.15360
9. Brunner L, Schaller N, Anstey J, Sillmann J, Steiner AK (2018) Dependence of Present and Future European Temperature Extremes on the Location of Atmospheric Blocking. Geophys Res Lett 45:6311–6320. https://doi.org/10.1029/2018GL077837
10. Buitenwerf R, Sandel B, Normand S, Mimet A, Svenning J-C (2018) Land surface greening suggests vigorous woody regrowth throughout European semi-natural vegetation. Glob Chang Biol 24:5789–5801. https://doi.org/10.1111/gcb.14451
11. Büntgen U, Urban O, Krusic PJ, Rybníček M, Kolář T, Kyncl T, Ač A, Koňasová E, Čáslavský J, Esper J, Wagner S, Saurer M, Tegel W, Dobrovolný P, Cherubini P, Reinig F, Trnka M (2021) Recent European drought extremes beyond Common Era background variability. Nat Geosci 14:190–196. https://doi.org/10.1038/s41561-021-00698-0

12. Burrell AL, Evans JP, de Kauwe MG (2020) Anthropogenic climate change has driven over 5 million km2 of drylands towards desertification. Nat Commun 11:3853. https://doi.org/10.1038/s41467-020-17710-7
13. Chan SC, Kahana R, Kendon EJ, Fowler HJ (2018) Projected changes in extreme precipitation over Scotland and Northern England using a high-resolution regional climate model. Clim Dyn 51:3559–3577. https://doi.org/10.1007/s00382-018-4096-4
14. Chen C, Park T, Wang X, Piao S, Xu B, Chaturvedi RK, Fuchs R, Brovkin V, Ciais P, Fensholt R, Tømmervik H, Bala G, Zhu Z, Nemani RR, Myneni RB (2019) China and India lead in greening of the world through land-use management. Nat Sustain 2:122–129. https://doi.org/10.1038/s41893-019-0220-7
15. Christian JI, Basara JB, Hunt ED, Otkin JA, Xiao X (2020) Flash drought development and cascading impacts associated with the 2010 Russian heatwave. Environ Res Lett 15:94078. https://doi.org/10.1088/1748-9326/ab9faf
16. Christidis N, McCarthy M, Cotterill D, Stott PA (2021) Record-breaking daily rainfall in the United Kingdom and the role of anthropogenic forcings. Atmos Sci Lett 22. https://doi.org/10.1002/asl.1033
17. Ciais P, Reichstein M, Viovy N, Granier A, Ogée J, Allard V, Aubinet M, Buchmann N, Bernhofer C, Carrara A, Chevallier F, de Noblet N, Friend AD, Friedlingstein P, Grünwald T, Heinesch B, Keronen P, Knohl A, Krinner G, Loustau D, Manca G, Matteucci G, Miglietta F, Ourcival JM, Papale D, Pilegaard K, Rambal S, Seufert G, Soussana JF, Sanz MJ, Schulze ED, Vesala T, Valentini R (2005) Europe-wide reduction in primary productivity caused by the heat and drought in 2003. Nature 437:529–533. https://doi.org/10.1038/nature03972
18. Cortés J, Mahecha MD, Reichstein M, Myneni RB, Chen C, Brenning A (2021) Where Are Global Vegetation Greening and Browning Trends Significant? Geophys Res Lett 48:1585. https://doi.org/10.1029/2020GL091496
19. Cramer W, Guiot J, Fader M, Garrabou J, Gattuso J-P, Iglesias A, Lange MA, Lionello P, Llasat MC, Paz S, Peñuelas J, Snoussi M, Toreti A, Tsimplis MN, Xoplaki E (2018) Climate change and interconnected risks to sustainable development in the Mediterranean. Nat Clim Chang 8:972–980. https://doi.org/10.1038/s41558-018-0299-2
20. Dai A, Trenberth KE, Karl TR (1998) Global variations in droughts and wet spells: 1900–1995. Geophys Res Lett 25:3367–3370. https://doi.org/10.1029/98GL52511
21. de Jong R, Verbesselt J, Schaepman ME, Bruin S (2012) Trend changes in global greening and browning: contribution of short-term trends to longer-term change. Glob Chang Biol 18:642–655. https://doi.org/10.1111/j.1365-2486.2011.02578.x
22. Del Martinez Castillo E, Zang CS, Buras A, Hacket-Pain A, Esper J, Serrano-Notivoli R, Hartl C, Weigel R, Klesse S, Resco de Dios V, Scharnweber T, Dorado-Liñán I, van der Maaten-Theunissen M, van der Maaten E, Jump A, Mikac S, Banzragch B-E, Beck W, Cavin L, Claessens H, Čada V, Čufar K, Dulamsuren C, Gričar J, Gil-Pelegrín E, Janda P, Kazimirovic M, Kreyling J, Latte N, Leuschner C,

Longares LA, Menzel A, Merela M, Motta R, Muffler L, Nola P, Petritan AM, Petritan IC, Prislan P, Rubio-Cuadrado Á, Rydval M, Stajić B, Svoboda M, Toromani E, Trotsiuk V, Wilmking M, Zlatanov T, de Luis M (2022) Climate-change-driven growth decline of European beech forests. Commun Biol 5:163. https://doi.org/10.1038/s42003-022-03107-3

23. Di Capua G, Sparrow S, Kornhuber K, Rousi E, Osprey S, Wallom D, van den Hurk B, Coumou D (2021) Drivers behind the summer 2010 wave train leading to Russian heatwave and Pakistan flooding. npj Clim Atmos Sci 4. https://doi.org/10.1038/s41612-021-00211-9
24. Di Paola A, Caporaso L, Di Paola F, Bombelli A, Vasenev I, Nesterova OV, Castaldi S, Valentini R (2018) The expansion of wheat thermal suitability of Russia in response to climate change. Land Use Policy 78:70–77. https://doi.org/10.1016/j.landusepol.2018.06.035
25. Dietze M, Bell R, Ozturk U, Cook KL, Andermann C, Beer AR, Damm B, Lucia A, Fauer FS, Nissen KM, Sieg T, Thieken AH (2022) More than heavy rain turning into fast-flowing water – a landscape perspective on the 2021 Eifel floods. EGUsphere. https://doi.org/10.5194/egusphere-2022-7
26. Dirmeyer PA, Balsamo G, Blyth EM, Morrison R, Cooper HM (2021) Land-Atmosphere Interactions Exacerbated the Drought and Heatwave Over Northern Europe During Summer 2018. AGU Adv 2:1. https://doi.org/10.1029/2020AV000283
27. Dye DG, Tucker CJ (2003) Seasonality and trends of snow-cover, vegetation index, and temperature in northern Eurasia. Geophys Res Lett 30. https://doi.org/10.1029/2002GL016384
28. Eckert S, Hüsler F, Liniger H, Hodel E (2015) Trend analysis of MODIS NDVI time series for detecting land degradation and regeneration in Mongolia. J Arid Environ 113:16–28. https://doi.org/10.1016/j.jaridenv.2014.09.001
29. Fay PA, Jin VL, Way DA, Potter KN, Gill RA, Jackson RB, Wayne Polley H (2012) Soil-mediated effects of subambient to increased carbon dioxide on grassland productivity. Nat Clim Chang 2:742–746. https://doi.org/10.1038/NCLIMATE1573
30. Fischer EM, Sippel S, Knutti R (2021) Increasing probability of record-shattering climate extremes. Nat Clim Chang 11:689–695. https://doi.org/10.1038/s41558-021-01092-9
31. Flanner MG, Zender CS, Hess PG, Mahowald NM, Painter TH, Ramanathan V, Rasch PJ (2009) Springtime warming and reduced snow cover from carbonaceous particles. Atmos Chem Phys 9:2481–2497. https://doi.org/10.5194/acp-9-2481-2009
32. Forkel M, Carvalhais N, Verbesselt J, Mahecha M, Neigh C, Reichstein M (2013) Trend Change Detection in NDVI Time Series: Effects of Inter-Annual Variability and Methodology. Remote Sens 5:2113–2144. https://doi.org/10.3390/rs5052113
33. Forzieri G, Alkama R, Miralles DG, Cescatti A (2017) Satellites reveal contrasting responses of regional climate to the widespread greening of Earth. Science 356:1180–1184. https://doi.org/10.1126/science.aal1727
34. Gampe D, Zscheischler J, Reichstein M, O'Sullivan M, Smith WK, Sitch S, Buermann W (2021) Increasing impact of warm droughts on northern ecosystem productivity over recent decades. Nat Clim Chang 11:772–779. https://doi.org/10.1038/s41558-021-01112-8

35. Geist HJ, Lambin EF (2004) Dynamic Causal Patterns of Desertification. Clim Res 54:817. https://doi.org/10.1641/0006-3568(2004)054[0817:DCPOD]2.0.CO;2
36. Godfray HCJ, Beddington JR, Crute IR, Haddad L, Lawrence D, Muir JF, Pretty J, Robinson S, Thomas SM, Toulmin C (2010) Food security: the challenge of feeding 9 billion people. Science 327:812–818. https://doi.org/10.1126/science.1185383
37. Gupta A, Rico-Medina A, Caño-Delgado AI (2020) The physiology of plant responses to drought. Science 368:266–269. https://doi.org/10.1126/science.aaz7614
38. Hari V, Rakovec O, Markonis Y, Hanel M, Kumar R (2020) Increased future occurrences of the exceptional 2018–2019 Central European drought under global warming. Sci Rep 10:12207. https://doi.org/10.1038/s41598-020-68872-9
39. Harris I, Osborn TJ, Jones P, Lister D (2020) Version 4 of the CRU TS monthly high-resolution gridded multivariate climate dataset. Sci Data 7:109. https://doi.org/10.1038/s41597-020-0453-3
40. Harris RB (2010) Rangeland degradation on the Qinghai-Tibetan plateau: A review of the evidence of its magnitude and causes. J Arid Environ 74:1–12. https://doi.org/10.1016/j.jaridenv.2009.06.014
41. Herrmann SM, Anyamba A, Tucker CJ (2005) Recent trends in vegetation dynamics in the African Sahel and their relationship to climate. Glob Environ Change 15:394–404. https://doi.org/10.1016/j.gloenvcha.2005.08.004
42. Herrmann SM, Hutchinson CF (2005) The changing contexts of the desertification debate. J Arid Environ 63:538–555. https://doi.org/10.1016/j.jaridenv.2005.03.003
43. Herrmann SM, Tappan GG (2013) Vegetation impoverishment despite greening: A case study from central Senegal. J Arid Environ 90:55–66. https://doi.org/10.1016/j.jaridenv.2012.10.020
44. Ibrahim YZ, Balzter H, Kaduk J (2018) Land degradation continues despite greening in the Nigeria-Niger border region. Global Ecol Conserv 16:e00505. https://doi.org/10.1016/j.gecco.2018.e00505
45. Justice CO, Townshend JRG, Holben BN, Tucker CJ (1985) Analysis of the phenology of global vegetation using meteorological satellite data. Int J Remote Sens 6:1271–1318. https://doi.org/10.1080/01431168508948281
46. Kaczan DJ, Orgill-Meyer J (2020) The impact of climate change on migration: a synthesis of recent empirical insights. Clim Change 158:281–300. https://doi.org/10.1007/s10584-019-02560-0
47. Kahle M, Glaser R, Kempf M (2022) Tracking the 2021 Central European flood event through text-mining and instrumental data analyses. Environmental Research Communications. (under review)
48. Kempf M, Glaser R (2020) Tracing Real-Time Transnational Hydrologic Sensitivity and Crop Irrigation in the Upper Rhine Area over the Exceptional Drought Episode 2018–2020 Using Open Source Sentinel-2 Data. Water 12:3298. https://doi.org/10.3390/w12123298
49. Ketzler G, Römer W, Beylich AA (2021) The Climate of Norway. In: Beylich AA (ed) Landscapes and Landforms of Norway. Springer International Publishing, Cham, pp 7–29
50. Klesse S, Babst F, Lienert S, Spahni R, Joos F, Bouriaud O, Carrer M, Di Filippo A, Poulter B, Trotsiuk V, Wilson R, Frank DC (2018) A Combined Tree Ring and Vegetation Model Assessment of European

Forest Growth Sensitivity to Interannual Climate Variability. https://doi.org/10.1029/2017GB005856. Global Biogeochem. Cycles

51. Kumar S, Peters-Lidard C, Tian Y, Houser P, Geiger J, Olden S, Lighty L, Eastman J, Doty B, Dirmeyer P (2006) Land information system: An interoperable framework for high resolution land surface modeling. Environ Model Softw 21:1402–1415. https://doi.org/10.1016/j.envsoft.2005.07.004
52. Lambin EF, Geist HJ (2006) Land-Use and Land-Cover Change: Local Processes and Global Impacts. Global Change - the IGBP Ser. Springer, Berlin / Heidelberg, Berlin, Heidelberg
53. Lesk C, Rowhani P, Ramankutty N (2016) Influence of extreme weather disasters on global crop production. Nature 529:84–87. https://doi.org/10.1038/nature16467
54. Li Z, Huffman T, McConkey B, Townley-Smith L (2013) Monitoring and modeling spatial and temporal patterns of grassland dynamics using time-series MODIS NDVI with climate and stocking data. Remote Sens Environ 138:232–244. https://doi.org/10.1016/j.rse.2013.07.020
55. Lin M, Horowitz LW, Xie Y, Paulot F, Malyshev S, Shevliakova E, Finco A, Gerosa G, Kubistin D, Pilegaard K (2020) Vegetation feedbacks during drought exacerbate ozone air pollution extremes in Europe. Nat Clim Chang 10:444–451. https://doi.org/10.1038/s41558-020-0743-y
56. Liu X, He B, Guo L, Huang L, Chen D (2020) Similarities and Differences in the Mechanisms Causing the European Summer Heatwaves in 2003, 2010, and 2018. Earths Future 8. https://doi.org/10.1029/2019EF001386
57. Luterbacher J, Dietrich D, Xoplaki E, Grosjean M, Wanner H (2004) European seasonal and annual temperature variability, trends, and extremes since 1500. Science 303:1499–1503. https://doi.org/10.1126/science.1093877
58. Masson-Delmotte V, Zhai, P, Pirani A, Connors SL, Péan C, Berger SB, Caud N, Chen Y, Goldfarb L, Gomis MI, Huang M, Leitzell K, Lonnoy E, Matthews J, Maycock TK, Waterfield T, Yelekçi O, Yu R, Zhou B (eds) (2021) IPCC 2021: Climate Change 2021: The Physical Science Basis. Contribution of Working Group I to the Sixth Assessment Report of the Intergovernmental Panel on Climate Change. Cambridge University Press
59. Menzel A, Sparks T, Estrella N, Koch E, Aasa A, Ahas R, Alm-Kübler K, Bissolli P, Braslavská O, Briede A, Chmielewski F, Crepinsek Z, Curnel Y, Dahl Ã, Defila C, Donnelly A, Filella Y, Jatczak K, Mage F, Mestre A, Nordli Ø, Penuelas J, Pirinen P, Remisova V, Scheifinger H, Striz M, Susnik A, van Vliet AJH, Wielgolaski F-E, Zach S, Zust A (2006) European phenological response to climate change matches the warming pattern. Glob Chang Biol 12:1969–1976. https://doi.org/10.1111/j.1365-2486.2006.01193.x
60. Menzel A, Yuan Y, Matiu M, Sparks T, Scheifinger H, Gehrig R, Estrella N (2020) Climate change fingerprints in recent European plant phenology. Glob Chang Biol. https://doi.org/10.1111/gcb.15000
61. Miralles DG, Teuling AJ, van Heerwaarden CC, Vilà-Guerau de Arellano J (2014) Mega-heatwave temperatures due to combined soil desiccation and atmospheric heat accumulation. Nat Geosci 7:345–349. https://doi.org/10.1038/NGEO2141

62. Myers-Smith IH, Kerby JT, Phoenix GK, Bjerke JW, Epstein HE, Assmann JJ, John C, Andreu-Hayles L, Angers-Blondin S, Beck PSA, Berner LT, Bhatt US, Bjorkman AD, Blok D, Bryn A, Christiansen CT, Cornelissen JHC, Cunliffe AM, Elmendorf SC, Forbes BC, Goetz SJ, Hollister RD, de Jong R, Loranty MM, Macias-Fauria M, Maseyk K, Normand S, Olofsson J, Parker TC, Parmentier F-JW, Post E, Schaepman-Strub G, Stordal F, Sullivan PF, Thomas HJD, Tømmervik H, Treharne R, Tweedie CE, Walker DA, Wilmking M, Wipf S (2020) Complexity revealed in the greening of the Arctic. Nat Clim Chang 10:106–117. https://doi.org/10.1038/s41558-019-0688-1
63. Peng X, Zhang T, Frauenfeld OW, Wang S, Qiao L, Du R, Mu C (2020) Northern Hemisphere Greening in Association With Warming Permafrost. J Geophys Res Biogeosci 125:2742. https://doi.org/10.1029/2019JG005086
64. Pereira SC, Marta-Almeida M, Carvalho AC, Rocha A (2017) Heat wave and cold spell changes in Iberia for a future climate scenario. Int J Climatol 37:5192–5205. https://doi.org/10.1002/joc.5158
65. Peters-Lidard CD, Houser PR, Tian Y, Kumar SV, Geiger J, Olden S, Lighty L, Doty B, Dirmeyer P, Adams J, Mitchell K, Wood EF, Sheffield J (2007) High-performance Earth system modeling with NASA/GSFC's Land Information System. Innovations Syst Softw Eng 3:157–165. https://doi.org/10.1007/s11334-007-0028-x
66. Piao S, Liu Q, Chen A, Janssens IA, Fu Y, Dai J, Liu L, Lian X, Shen M, Zhu X (2019) Plant phenology and global climate change: Current progresses and challenges. Glob Chang Biol 25:1922–1940. https://doi.org/10.1111/gcb.14619
67. Piao S, Wang X, Park T, Chen C, Lian X, He Y, Bjerke JW, Chen A, Ciais P, Tømmervik H, Nemani RR, Myneni RB (2020) Characteristics, drivers and feedbacks of global greening. Nat Rev Earth Environ 1:14–27. https://doi.org/10.1038/s43017-019-0001-x
68. Pierce D (2019) ncdf4: Interface to Unidata netcdf (Version 4 or Earlier) Format Data Files. http://cirrus.ucsd.edu/~pierce/ncdf
69. Piticar A, Croitoru A-E, Ciupertea F-A, Harpa G-V (2018) Recent changes in heat waves and cold waves detected based on excess heat factor and excess cold factor in Romania. Int J Climatol 38:1777–1793. https://doi.org/10.1002/joc.5295
70. Pool S, Francés F, Garcia-Prats A, Pulido-Velazquez M, Sanchis-Ibor C, Schirmer M, Yang H, Jiménez-Martínez J (2021) From Flood to Drip Irrigation Under Climate Change: Impacts on Evapotranspiration and Groundwater Recharge in the Mediterranean Region of Valencia (Spain). Earths Future 9. https://doi.org/10.1029/2020EF001859
71. Quesada B, Vautard R, Yiou P, Hirschi M, Seneviratne SI (2012) Asymmetric European summer heat predictability from wet and dry southern winters and springs. Nat Clim Chang 2:736–741. https://doi.org/10.1038/NCLIMATE1536
72. Rasmijn LM, van der Schrier G, Bintanja R, Barkmeijer J, Sterl A, Hazeleger W (2018) Future equivalent of 2010 Russian heatwave intensified by weakening soil moisture constraints. Nat Clim Chang 8:381–385. https://doi.org/10.1038/s41558-018-0114-0

73. Rodell M, Houser PR, Jambor U, Gottschalck J, Mitchell K, Meng C-J, Arsenault K, Cosgrove B, Radakovich J, Bosilovich M, Entin JK, Walker JP, Lohmann D, Toll D (2004) The Global Land Data Assimilation System. Bull Amer Meteor Soc 85:381–394. https://doi.org/10.1175/BAMS-85-3-381
74. Rosbakh S, Hartig F, Sandanov DV, Bukharova EV, Miller TK, Primack RB (2021) Siberian plants shift their phenology in response to climate change. Glob Chang Biol 27:4435–4448. https://doi.org/10.1111/gcb.15744
75. Schmidhuber J, Tubiello FN (2007) Global food security under climate change. Proc Natl Acad Sci U S A 104:19703–19708. https://doi.org/10.1073/pnas.0701976104
76. Schumacher DL, Keune J, van Heerwaarden CC, Vilà-Guerau de Arellano J, Teuling AJ, Miralles DG (2019) Amplification of mega-heatwaves through heat torrents fuelled by upwind drought. Nat Geosci 12:712–717. https://doi.org/10.1038/s41561-019-0431-6
77. Sousa PM, Barriopedro D, García-Herrera R, Ordóñez C, Soares PMM, Trigo RM (2020) Distinct influences of large-scale circulation and regional feedbacks in two exceptional 2019 European heatwaves. Commun Earth Environ 1:857. https://doi.org/10.1038/s43247-020-00048-9
78. Tucker CJ (1979) Red and photographic infrared linear combinations for monitoring vegetation. Remote Sens Environ 8:127–150. https://doi.org/10.1016/0034-4257(79)90013-0
79. Tucker CJ, Fung IY, Keeling CD, Gammon RH (1986) Relationship between atmospheric CO2 variations and a satellite-derived vegetation index. Nature 319:195–199. https://doi.org/10.1038/319195a0
80. Tucker CJ, Newcomb WW, Los SO, Prince SD (1991) Mean and inter-year variation of growing-season normalized difference vegetation index for the Sahel 1981–1989. Int J Remote Sens 12:1133–1135. https://doi.org/10.1080/01431169108929717
81. Vogel E, Donat MG, Alexander LV, Meinshausen M, Ray DK, Karoly D, Meinshausen N, Frieler K (2019) The effects of climate extremes on global agricultural yields. Environ Res Lett 14:54010. https://doi.org/10.1088/1748-9326/ab154b
82. Vogel J, Paton E, Aich V, Bronstert A (2021) Increasing compound warm spells and droughts in the Mediterranean Basin. Weather and Climate Extremes 32:100312. https://doi.org/10.1016/j.wace.2021.100312
83. Whan K, Sillmann J, Schaller N, Haarsma R (2020) Future changes in atmospheric rivers and extreme precipitation in Norway. Clim Dyn 54:2071–2084. https://doi.org/10.1007/s00382-019-05099-z
84. Winkler AJ, Myneni RB, Hannart A, Sitch S, Haverd V, Lombardozzi D, Arora VK, Pongratz J, Nabel JEMS, Goll DS, Kato E, Tian H, Arneth A, Friedlingstein P, Jain AK, Zaehle S, Brovkin V (2021) Slowdown of the greening trend in natural vegetation with further rise in atmospheric CO_2. Biogeosciences 18:4985–5010. https://doi.org/10.5194/bg-18-4985-2021
85. Wu M, Vico G, Manzoni S, Cai Z, Bassiouni M, Tian F, Zhang J, Ye K, Messori G (2021) Early Growing Season Anomalies in Vegetation Activity Determine the Large-Scale Climate-Vegetation Coupling in Europe. J Geophys Res Biogeosci 126:157. https://doi.org/10.1029/2020JG006167

86. Xu Z, Cao L, Zhong S, Liu G, Yang Y, Zhu S, Luo X, Di L (2020) Trends in Global Vegetative Drought From Long-Term Satellite Remote Sensing Data. IEEE J Sel Top Appl Earth Observations Remote Sensing 13:815–826. https://doi.org/10.1109/JSTARS.2020.2972574
87. Zahradníček P, Trnka M, Brázdil R, Možný M, Štěpánek P, Hlavinka P, Žalud Z, Malý A, Semerádová D, Dobrovolný P, Dubrovský M, Řezníčková L (2015) The extreme drought episode of August 2011-May 2012 in the Czech Republic. Int J Climatol 35:3335–3352. https://doi.org/10.1002/joc.4211
88. Zhang R, Sun C, Zhu J, Zhang R, Li W (2020) Increased European heat waves in recent decades in response to shrinking Arctic sea ice and Eurasian snow cover. npj Clim Atmos Sci 3. https://doi.org/10.1038/s41612-020-0110-8
89. Zhang W, Furtado K, Wu P, Zhou T, Chadwick R, Marzin C, Rostron J, Sexton D (2021) Increasing precipitation variability on daily-to-multiyear time scales in a warmer world. Sci Adv 7. https://doi.org/10.1126/sciadv.abf8021
90. Zhou L, Tucker CJ, Kaufmann RK, Slayback D, Shabanov NV, Myneni RB (2001) Variations in northern vegetation activity inferred from satellite data of vegetation index during 1981 to 1999. J Geophys Res Atmos 106:20069–20083. https://doi.org/10.1029/2000JD000115
91. Zhou S, Williams AP, Berg AM, Cook BI, Zhang Y, Hagemann S, Lorenz R, Seneviratne SI, Gentine P (2019) Land-atmosphere feedbacks exacerbate concurrent soil drought and atmospheric aridity. Proc Natl Acad Sci U S A 116:18848–18853. https://doi.org/10.1073/pnas.1904955116
92. Zida WA, Bationo BA, Waaub J-P (2020) Re-greening of agrosystems in the Burkina Faso Sahel: greater drought resilience but falling woody plant diversity. Envir Conserv 47:174–181. https://doi.org/10.1017/S037689292000017X
93. Zolina O, Simmer C, Gulev SK, Kollet S (2010) Changing structure of European precipitation: Longer wet periods leading to more abundant rainfalls. Geophys Res Lett 37. https://doi.org/10.1029/2010GL042468

Figures

Figure 1

Spectral surface reflectance trends derived from annual NDVI composites (95% confidence level) compared to total precipitation and temperature trends (areas with 95% confidence level marked as black dots) across Europe for the period 2001-2020.

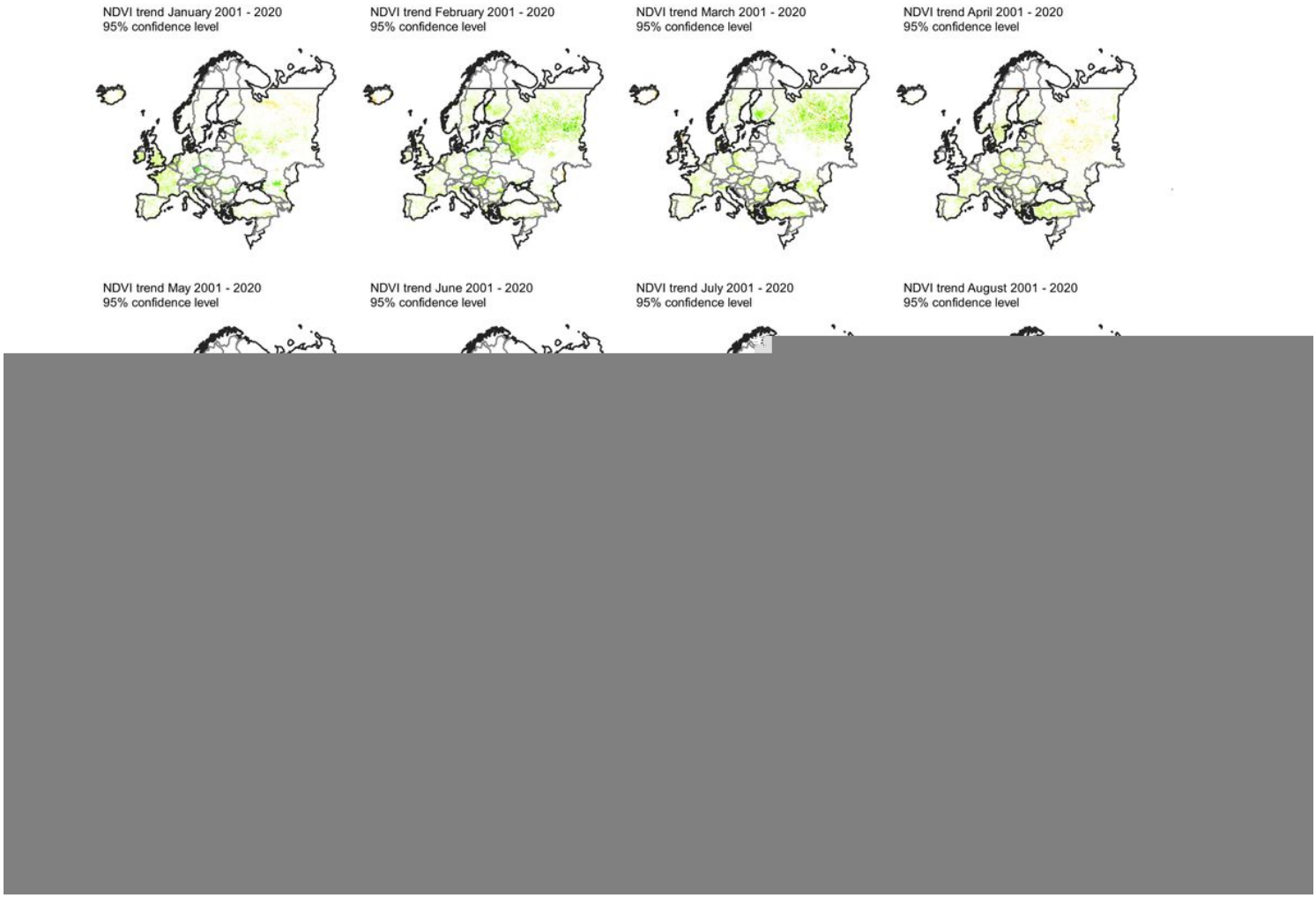

Figure 2

Multiannual monthly NDVI trends with 95% confidence level across Europe (2001-2020).

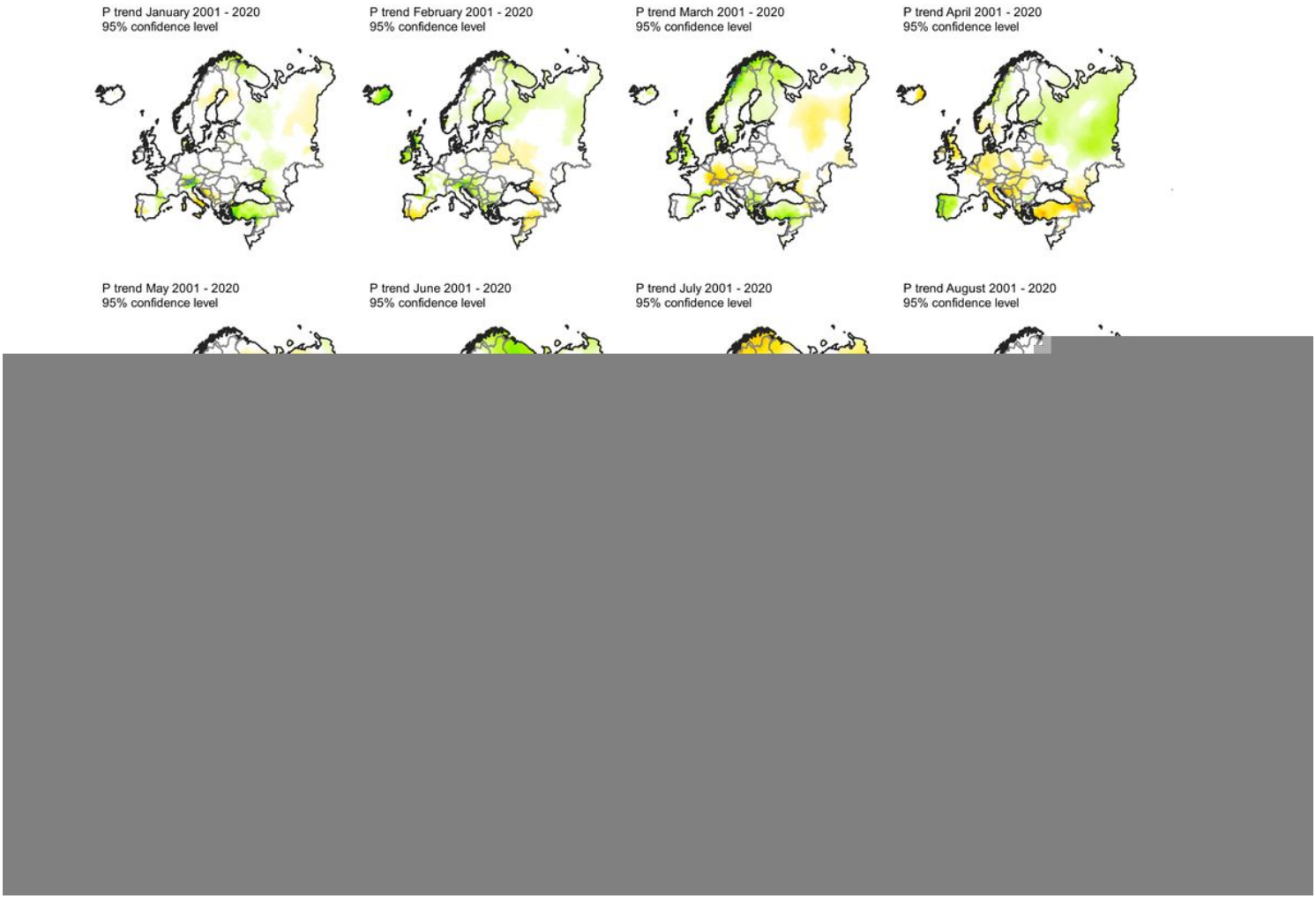

Figure 3

Multiannual monthly precipitation trends with 95% confidence level across Europe (2001-2020).

Figure 4

Multiannual monthly temperature trends with 95% confidence level across Europe (2001-2020).

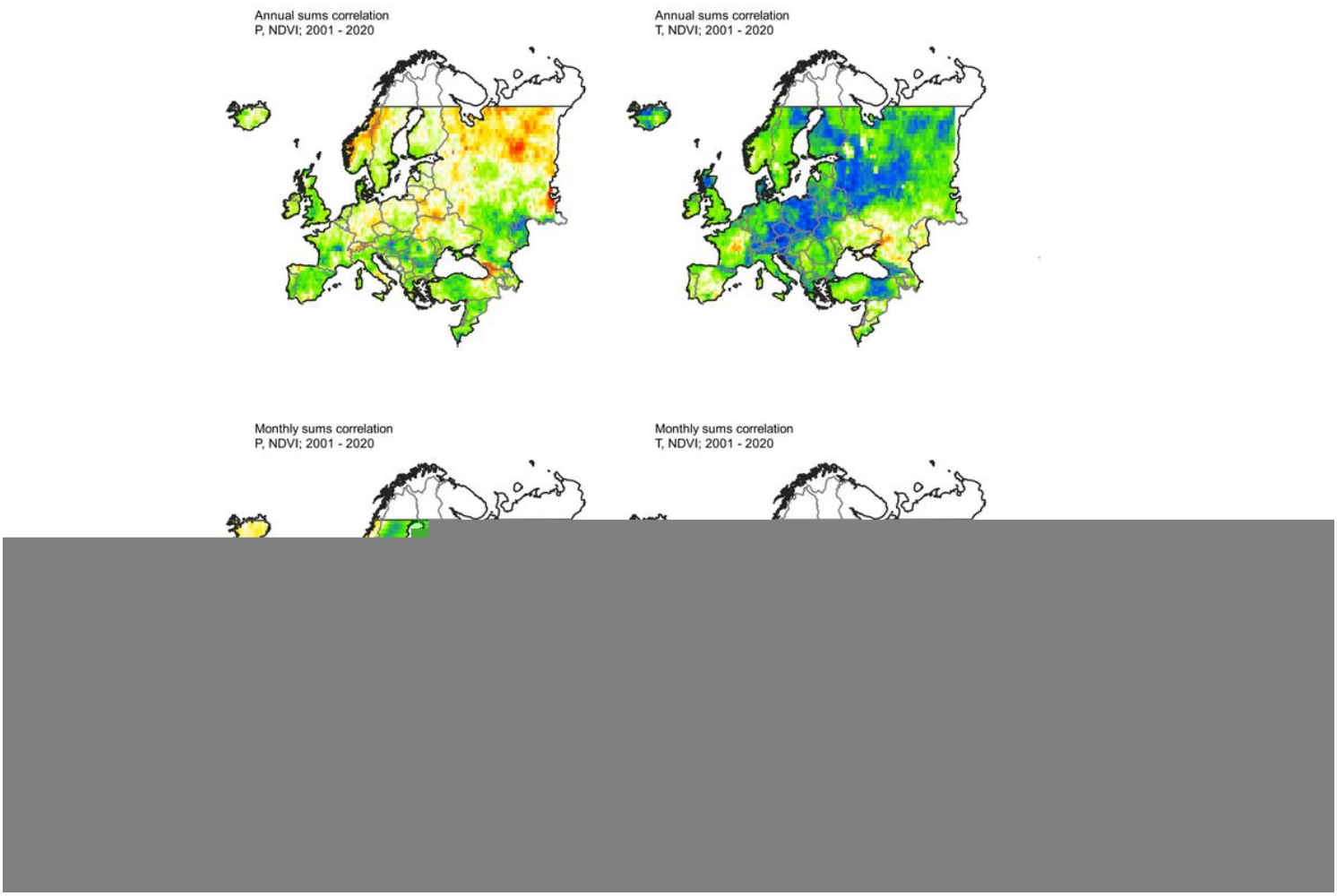

Figure 5

Correlation raster *(p-values*) of annual total precipitation and NDVI, annual average temperature and NDVI, and monthly composites over the period 2001-2020.

Figure 6

Correlation of NDVI and GLDAS variables as p-value raster and p-value box-/density plots (see Tab. 1 for labels).

Figure 7

Temperature, precipitation, and NDVI anomalies between 2001-2020 across Europe.

Supplementary Files

This is a list of supplementary files associated with this preprint. Click to download.

- 1Code1ReadandextractMODISNDVIhdf4data.r
- 3Code3prepareMODISEUcrops.r
- 4Code4createannualanomaliesfromrasterstacktimeseries.r
- 5Code5performtrendanalysisfromrastertimeseries.r
- 6Code6correlationbetweenNDVIandGLDASvariablesstacks.r
- 7Code7createposandneganomalyrastersums.r
- EUECanopTavgtrend2001202095percconf.tif
- EUEsoilTavgtrend2001202095percconf.tif
- EUEvapotranspiration trend2001202095percconf.tif
- EUPotEvapTavgtrend2001202095percconf.tif
- EURootMoistInsttrend2001202095percconf.tif
- EUSnowDepthMetertrend2001202095percconf.tif
- EUSnowDepthWaterEquivalenttrend2001202095percconf.tif
- EUSoilMoist010cmtrend2001202095percconf.tif
- EUSoilMoist100200cmtrend2001202095percconf.tif
- EUSoilMoist1040cmtrend2001202095percconf.tif
- EUSoilMoist40100cmtrend2001202095percconf.tif
- EUSoilTMP40100cmtrend2001202095percconf.tif
- EUSurfRunOfftrend2001202095percconf.tif
- EUSurfSnowMeltAmounttrend2001202095percconf.tif
- EUSurfaceSnowMelttrend2001202095percconf.tif
- EUTvegTavgtrend2001202095percconf.tif
- EUWindtrend2001202095percconf.tif